Supplementary Materials to the article

Ecological Resource Availability

–

A method to estimate resource budgets for a sustainable economy

Harald Desing*[1], Gregor Braun[1], Roland Hischier[1]

[1] Empa - Swiss Federal Laboratories for Material Science and Technology, Lerchenfeldstrasse 5, 9014 St. Gallen, Switzerland
* corresponding author: harald.desing@empa.ch

The supplementary material contain details on uncertainty modeling, translation of the planetary boundaries framework for the ERA method, the quantification of impacts from industrial sectors and their supply chains using Exiobase (Stadler et al., 2018), the quantification of environmental impacts from processes using ecoinvent (Wernet et al., 2016), a list of abbreviations and a glossary. The calculation code in Matlab (R2018) and necessary Excel-files are available online at https://doi.org/10.5281/zenodo.3629366.

Contents

1 Uncertainty modeling

No parameter is known with absolute certainty, due to inherent uncertainties of the system, such as e.g., statistical nature of real life chaotic problems, measurement errors, influence of observation on the system, and limitations of current scientific understanding and spatial and temporal variability. The latter group of uncertainties can be reduced through improved modeling (i.e., regionalization and dynamic modeling) and advances in scientific knowledge.

Each parameter in the Ecological Resource Availability (ERA) method is specified with an uncertainty range and assigned a probability density function (PDF) (Muller et al., 2014, 2016). A Monte-Carlo simulation (MC) is performed with $n_{\text{runs}} = 10^5$ simulation runs to consider the uncertainty of the parameters and the uncertainty propagation throughout the calculations. The calculation and simulation is performed in Matlab R2018. The advantage of a MC simulation over analytical calculations is, that different PDF and empirical data sets can be considered also in complex linear and non-linear systems. Each parameter is therefore picked randomly for each simulation run n_{runs} according to the PDF specified with the input parameters in table S1.

distribution	description	min	mode	max	d
beta-PERT	smooth PDF with absolute min and max	a	c	b	1
triangular	forms a triangle between $(min, p = 0), (mode, p(mode)), (max, p = 0)$ with $p(mode)$ so that $\int_{min}^{max} p = 1$	a	c	b	2
normal	Gaußian distribution	–	μ	$\mu + 3\sigma$	3
log-normal	ln-transformed Gaußian distribution	–	e^{μ}	$e^{\mu+3\sigma}$	4
uniform	each value between min and max has the same probability	min	–	max	5
balance coefficient	is determined as the residue to 1 for columns in a matrix. Only relevant, if the sum of each column in a matrix needs to equal 1	–	–	–	6

Table S1: Distributions to calculate random numbers for Monte-Carlo simulations.

The probability of violation is the area of overlap between the segment boundary (SB) and upscaled UI distributions. It is numerically calculated through counting the number of occurrences, that a load is greater than the strength and divided by the total number of runs.

$$P_{\text{v}} = \frac{1}{n_{\text{runs}}} \sum_{i=1}^{n_{\text{runs}}} \begin{cases} 1 & load \geq strength \\ 0 & load < strength \end{cases} \tag{1}$$

In the paper we set the acceptable risk of violation for the Earth System Boundaries (ESB) to $P_v = 0.01$. In current Earth system governance, this value is usually much higher (e.g. the climate change targets and trajectories limiting global warming to $< 2\,^{\circ}\text{C}$ are set with a confidence of $^2/_3$ (Myhre et al., 2013), i.e., there is a $^1/_3$ chance that the climate targets are not met even when the emission reduction targets are fulfilled); whereas for technical systems (see table S2), the probability for system failure is much lower.

2 Planetary boundaries translation, impact characterization and uncertainty

In this section, the boundary translation used in the case study is described in detail. The translation is based on and compared to multiple methods (fig. S1) (Doka, 2016; Ryberg et al., 2018; Chandrakumar et al., 2018; Dao et al., 2015; Meyer and Newman, 2018; Bjørn and Hauschild, 2015; EEA and FOEN, 2020). The translated boundaries have to be measurable in the EE-IOT exiobase v.3 (Tukker et al., 2009, 2014; Stadler et al., 2018) and LCA database ecoinvent v.3.5 (Wernet et al., 2016).

Engineering field	p_f / $^1/_h$	t_L / h	P_f	Description
Automotive structure (Heuler et al., 2010)	10^{-5}	10^3	10^{-2}	Failure of structural components lead to a serious accident
Aircraft engine, critical system (Hupfer, 2011)	10^{-7}	10^4	10^{-3}	Hazardous engine defects could potentially lead to a crash
Ship hull (Molland, 2008)	10^{-8}	10^5	10^{-3}	Cracking of the hull due to wave loads will lead to sinking of the ship
Nuclear power plant (Volkmer, 2007)	10^{-10}	10^5	10^{-5}	Melting of the core can have major and long lasting effects on the environment and society

Table S2: Typical probabilities of failure used in engineering. Probability density per operating time of failure p_f; service lifetime t_L; probability of failure over service life P_f.

2.1 Climate change

2.1.1 Atmospheric CO_2 concentration

The first control variable defines the atmospheric concentration of $c_{CO_2} < [350, 450]$ ppm (Steffen et al., 2015). CO_2 emissions are well reported in LCA and EE-IOT, however in units of mass, not concentration change. Ryberg et al. (2018) proposes to translate CO_2 emissions into CO_2 concentration change with a characterisation factor based on a 300 a time horizon. This factor can be used to calculate the annual emission allowance in starting from a reference concentration. Taking the pre-industrial concentration of 278 ppm, translates to annual emissions of $\dot{m}_{CO_2} = [2.68, 6.39]^{Pg/a}$; whereas taking the current concentration (414 ppm)[1] as a reference, allowed annual emissions are $\dot{m}_{CO_2} = [-2.38, 1.43]^{Pg/a}$. Meyer and Newman (2018) set the boundary based on a transition pathway scenario, where the target concentration of 350 ppm is reached in 2100. As a boundary, they take the negative emissions required in this pathway between 2050 and 2080: $\dot{m}_{CO_2} = -7.3^{Pg/a}$ (no uncertainty specified). All other authors do not translate this boundary.

Because the boundary settings from Ryberg et al. (2018) and Meyer and Newman (2018) are set with limited and specific time horizons, they do not correspond well with the scope of the ERA method. Therefore, we propose an alternative translation. The ERA method quantifies resource use at the level where the Holocene-like state of the Earth system can be maintained over time. This requires, that the atmospheric CO_2 concentration remains constant at the level specified in the PB. If the concentration is not to change, the inflow into the compartment "atmosphere" can only be as large as the corresponding outflow. Therefore, as much fossil CO_2 can be emitted per year as is absorbed by oceans and soils each year. The atmospheric CO_2 balance (Sarmiento and Gruber, 2006) can be expressed as:

$$\frac{dN}{dt} = F_{\text{natural}} + F_{\text{fossil}} + F_{\text{LUC}} + F_{\text{a/s}} + F_{\text{a/b}} + F_{\text{sediment}} \quad (2)$$

N	number of CO_2 molecules in the atmosphere
F_{natural}	emission of CO_2 by natural events, like volcanism or weathering
F_{fossil}	emission of CO_2 from fossil sources
F_{LUC}	emission of CO_2 due to land use change (LUC)
$F_{\text{a/s}}$	net exchange of CO_2 at the atmosphere - sea interface, minus weathering
$F_{\text{a/b}}$	net exchange of CO_2 between the atmosphere and biosphere, minus LUC and weathering
F_{sediment}	burial of carbon in sediments at the seafloor

In a steady state, the number of molecules of CO_2 in the atmosphere needs to be constant ($\frac{dN}{dt} = 0$) as well as no LUC may occur ($F_{\text{LUC}} = 0$). Further, both the net exchanges between atmosphere and sea as well as with the biosphere are close to zero over long time horizons. According to assessment report 5 of

[1] https://www.esrl.noaa.gov/gmd/ccgg/trends/global.html, accessed 17.7.2020

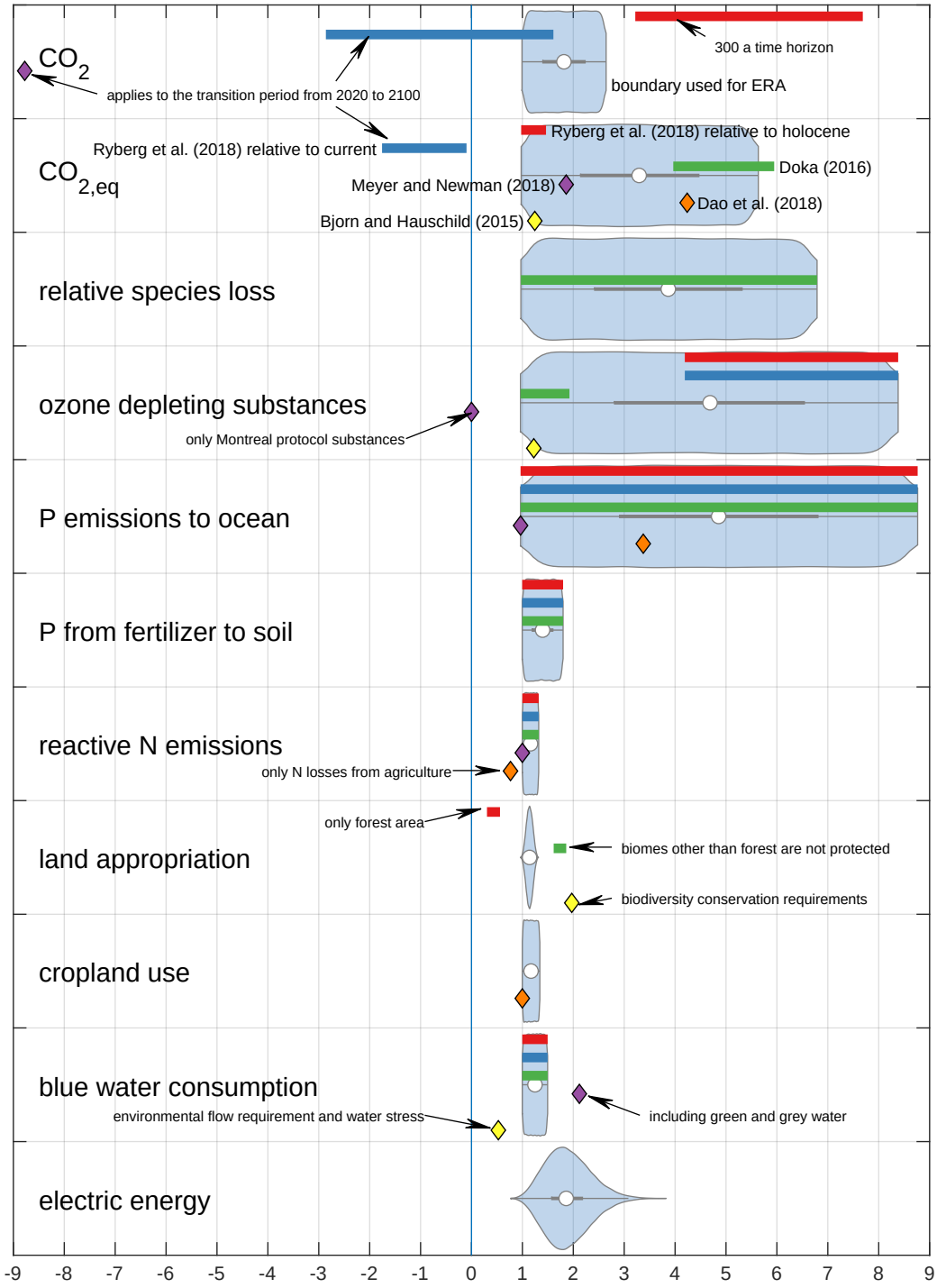

Figure S1: Comparison of ESB used in this case study (blue violins) to the translation using characterisation factors from Ryberg et al. (2018) relative to the holocene state of the Earth system (red bars) and relative to the current state (blue bars), translations done by (Doka, 2016) (green bars) and single boundary values from Meyer and Newman (2018) (violet diamond), Dao et al. (2018) (orange diamond) and Bjørn and Hauschild (2015) (yellow diamond). All values are normalized to the 0.5 % value of the boundary's uncertainty distribution as considered in the case study (=1).

IPCC (IPCC, 2013) the residence time of carbon in different compartments (e.g., soil, biomass, deep ocean, etc.) is within a human's lifetime (< 100 a) or within the perspective of civilizations (10^3 a) with only one exception: sediments. The residence time of C in sediments is $> 10^4$ a and thus the only compartment, which can be considered as a final sink in a human perspective.

The natural volcanic emission rate is about $< 0.36\,\mathrm{Pg/a}$ (CO_2) is compensated by net weathering of about $-0.72\,\mathrm{Pg/a}$ (CO_2) (IPCC, 2013), resulting in a net natural uptake of $F_{\mathrm{natural,CO_2}} = -0.36\,\mathrm{Pg/a}$. Additionally, there is a sedimentation rate of organic carbon $F_{\mathrm{sediment,CO_2}} = -0.72\,\mathrm{Pg/a}$. Volcanic emissions, sedimentation and weathering had been relatively constant over recent Earth history (IPCC, 2013). An examination of sediment bore cores from deep sea sites had found a variability of the sedimentation rate of about $\frac{F_{\mathrm{sediment}}(t)}{F_{\mathrm{sediment,today}}} = [0.624, 2.5]$ over the last 20 Ma (Stein, 1991). During the same time period, the atmospheric concentration of CO_2 had been below 450 ppm (IPCC, 2013), i.e., within or below the uncertainty interval of the boundary value specified by the PB framework (Rockström et al., 2009). Applying this variation on the sedimentation rate and adding the net removal through weathering processes, the fossil CO_2 emission rate can be determined.

$$F_{\mathrm{fossil,CO_2}} = [0.825, 2.2]\,\mathrm{Pg/a} \tag{3}$$

Please note, negative emissions will be necessary to reach the target CO_2 concentration during the transition. The Meyer and Newman (2018) boundary is therefore a good estimate for the efforts in the transition, however not a goal that will be relevant for beyond the transition. Future-proof products and services need to be designed for the time after the transition, acknowledging that during the transition extra efforts are necessary (e.g. CCS). Besides that, negative boundaries will lead to meaningless results in the ERA method when using a grandfathering approach, because ERA budgets will be negative. In scenarios allowing for CO_2 removing technologies and materials, a negative boundary can be implemented in the method.

2.1.2 Energy imbalance at top of the atmosphere

The second climate change boundary is defined as $< [1, 1.5]\,\mathrm{W/m^2}$ energy imbalance at the top of the atmosphere relative to pre-industrial levels (Steffen et al., 2015). This control variable accounts for the warming effect of CO_2 and other greenhouse gases (GHG) (e.g., CH_4, CO, aerosol loading). The GWP is usually described in LCIA in terms of emissions of mass of CO_2-equivalents. Doka (2016) relates the two units using the conversion factor $8.69 \times 10^{-14}\,\mathrm{Wa/m^2kg}$ for the GWP for a 100 a time horizon, which translates the boundary into $\dot{m}_{\mathrm{CO_2-eq}} = [1.09, 1.64] \times 10^{13}\,\mathrm{kg/a}$. The same procedure with the updated conversion factor $[9.17] \times 10^{-14}\,\mathrm{Wa/m^2kg}$ from Myhre et al. (2013) translates the boundary into $\dot{m}_{\mathrm{CO_2-eq}} = [1.09, 1.64] \times 10^{13}\,\mathrm{kg/a}$. Ryberg et al. (2018) applies again a 300 a time horizon for the conversion, which yields a boundary of $\dot{m}_{\mathrm{CO_2-eq}} = [2.83, 4.25] \times 10^{12}\,\mathrm{kg/a}$ in comparison to pre-industrial times; and $\dot{m}_{\mathrm{CO_2-eq}} = [-5.1, -0.28] \times 10^{12}\,\mathrm{kg/a}$ in comparison to current energy imbalance given by Steffen et al. (2015). Meyer and Newman (2018) only consider CH_4 and N_2O emissions for this boundary and set their boundary in $CO_{2,\mathrm{eq}}$ to $\dot{m}_{\mathrm{CO_2-eq}} = 1.23 \times 10^{13}\,\mathrm{kg/a}$. Dao et al. (2015) based their boundary on spreading the remaining carbon budget to stay $< 2\,^{\circ}\mathrm{C}$ with 50 % confidence (IPCC, 2013) over the years 2015 to 2100. Chandrakumar et al. (2018), in contrast, calculates a boundary to $\dot{m}_{\mathrm{CO_2-eq}} = 3 \times 10^{13}\,\mathrm{kg/a}$ based on the conversion factor from Doka (2016) but using the $2.6\,\mathrm{W/m^2}$ irradiation imbalance from IPCC scenarios limiting global warming to $< 2\,^{\circ}\mathrm{C}$ (IPCC, 2013), which is not in line with the PB. Bjørn and Hauschild (2015) propose a boundary for GWP100 of $\dot{m}_{\mathrm{CO_2-eq}} = 3.61 \times 10^{12}\,\mathrm{kg/a}$ based on a weighting of GHG relative to the climate change indicator score in 2010 and the $1\,\mathrm{W/m^2}$ boundary.

As a boundary for our case study, we take the lower uncertainty value from Ryberg et al. (2018) (relative to pre-industrial) and the upper value from Doka (2016) (with the updated conversion factor from IPCC (2013), i.e. $\dot{m}_{\mathrm{CO_2-eq}} = [2.83, 16.4] \times 10^{12}\,\mathrm{kg/a}$. In this way, the uncertainty range covers all reviewed studies, except for Ryberg et al. (2018) relative to current state, which is out of the scope for this method, and Chandrakumar et al. (2018), which is not in line with the original boundary. Please note, most GHG other than CO_2 have a lifetime in the atmosphere of <100 years. And because we already have considered the longer lifetime of CO_2 in the first boundary above, it justifies to set this boundary with commonly used time horizons (100 a and 300 a).

In order to quantify GWP from inventory results, various LCIA methods are available. To account for different modelling approaches (e.g., time horizon) and variations among impact assessment methods, a

rectangular distribution is formed with the minimum and maximum values among the following LCIA methods: CML 2001, ILCD 2.0 2018, IPCC 2007, IPCC 2013, ReCiPe V1.13 2016. The impact results are multiplied with the underlying inventory uncertainty (as modeled for the direct CO_2 emissions, but normalized to one as the geometric mean) to result in the total uncertainty range.

2.2 Change of biosphere integrity

The loss of biodiversity is of growing concern (European Commission, 2011; IPBES, 2019), however the control variables of the PB framework are only of preliminary character (Rockström et al., 2009; Steffen et al., 2015) and debated (Montoya et al., 2018; Newbold et al., 2016; Mace et al., 2014). One control variable defines the extinction rate as $[10, 100]\,{}^{\text{extinctions}}/_{10^6 \text{species}\cdot\text{a}}$, whereas the second defines the relative species abundance, or biodiversity intactness index (Scholes and Biggs, 2005), to $BII > [0.9, 0.3]$. Doka (2016) provides an approach for the latter, taking the *potentially disappeared fraction of species* (Goedkoop et al., 2013; Huijbregts et al., 2017; Doka, 2016; Verones et al., 2017) used in the LCIA method ReCiPe version 1.13 (Goedkoop et al., 2013; Huijbregts et al., 2017). To end up with relative species loss, *potentially disappeared fraction of species* needs to be multiplied with the species density, i.e., the total number of species on Earth. ReCiPe characterization factors are built with an approximate 1.95×10^6 number of known species(Goedkoop et al., 2013). Therewith the boundary can be translated to $[1.95, 13.7] \times 10^5$. Note, this value is specific to ReCiPe, it however indicates the global pressure on species loss correctly (IPBES, 2019) and can be easily implemented in ecoinvent and Exiobase. Meyer and Newman (2018) propose a different metric to evaluate the biodiversity boundary with the *percentage of disappeared fraction of species* of $< 1 \times 10^{-4}\,{}^{1}/_{\text{a}}$, whereas Dao et al. (2015) propose to use the biodiversity damage potential (boundary < 0.16). For simplicity, we use the approach from Doka (2016), as it can easily be implemented in ecoinvent and Exiobase. However, we stress the fact, that a more suitable boundary needs to be defined in accordance with state-of-the-art methods (e.g. UNEP and SETAC (2016)) assessing biodiversity impacts.

Different impact pathways lead to species loss (e.g., land occupation). The endpoint category of species loss is calculated from various midpoint indicators in ReCiPe (Goedkoop et al., 2013; Huijbregts et al., 2017). The impact pathways considered are climate change, land occupation, ecotoxicity, eutrophication, terrestrial acidification, water depletion for marine, freshwater and terrestrial ecosystems. The uncertainty range for the impact characterization is modeled as a uniform distribution with the minimum and maximum value from the three different scenarios in ReCiPe (i.e., hierarchic, egalitarian, individualist) multiplied with the uncertainty of the dominating inventory result (i.e., agricultural land occupation). Note, a more precise uncertainty range should be modeled using all different contributing inventory results and impact pathways (midpoints), which is simplified here for the first proof of concept of the method.

2.3 Stratospheric ozone depletion

Ozone depletion was among the first environmental problems successfully tackled by international commitment (Velders et al., 2007). Still, it remains important to observe the boundary in the future, as not all ozone depleting substances (ODS) can be banned. The PB is defined as a permitted loss of O_3 concentration of $-\Delta c_{O_3} = [14.5, 29]\,\text{DU}$ (DU = Dobson units).

Doka (2016) translates the O_3 concentration loss into emissions of substances with ozone depleting potential (ODP) with a conversion factor of $-\frac{\Delta c_{O_3}}{\dot{m}_{\text{CFC}-11-\text{eq}}} = 3.42 \times 10^{-8}\,{}^{\text{DU}\cdot\text{a}}/_{\text{kg}}$, leading to a boundary of $\dot{m}_{\text{CFC}-11,\text{eq}} = [4.24, 8.48] \times 10^8\,{}^{\text{kg}}/_{\text{a}}$. Ryberg et al. (2018) uses a different conversion factor of $-\frac{\Delta c_{O_3}}{\dot{m}_{\text{CFC}-11-\text{eq}}} = 7.85 \times 10^{-9}\,{}^{\text{DU}\cdot\text{a}}/_{\text{kg}}$, which translates to a boundary of $\dot{m}_{\text{CFC}-11,\text{eq}} = [1.85, 3.69] \times 10^9\,{}^{\text{kg}}/_{\text{a}}$. The factors consider the average effect of the emission of ODP on the reduction of O_3 concentration. Bjørn and Hauschild (2015) proposes a boundary of $\dot{m}_{\text{CFC}-11,\text{eq}} = 5.39 \times 10^8\,{}^{\text{kg}}/_{\text{a}}$, which is within the uncertainty range of Doka (2016). Meyer and Newman (2018) set their boundary to zero, however, it applies to substances regulated by the Montreal protocol only (does not include e.g. N_2O).

For the case study, we set the boundary to $\dot{m}_{\text{CFC}-11-\text{eq}} = [4.24, 36.9] \times 10^8\,{}^{\text{kg}}/_{\text{a}}$ using the lower value from Doka (2016) and the higher value from Ryberg et al. (2018). Ozone depleting substances (ODS) are commonly measured in LCIA in the ODP-eqivalent CFC-11-eq. The uncertainty range for the impact assessment is modeled as uniform distribution with the minimum and maximum vales from the following impact methods: CML 2001, ILCD 2.0 2018 and ReCiPe V1.13 2016.

2.4 Ocean acidification

CO_2 uptake of the oceans from the atmosphere is the main driver for the change in pH value in the oceans' surface water. This change leads to dissolving the shells of marine species. To prevent this, the ocean surface saturation state of aragonite needs to stay $\Omega_{\text{arag}} \geq [0.8, 0.7]$.

As the boundary is directly dependent on the climate change boundary, it is not operationalized in this method as it is expected, that if the CO_2 boundary is respected, so is the one for ocean acidification (Doka, 2016; Steffen et al., 2015).

2.5 Biogeochemical flows

2.5.1 Phosphorus to oceans

Phosphorus intake to oceans disturbs the nutrient balance and can lead to anoxic zones (Rockström et al., 2009), thus the global flow of P into ocean needs to be restricted to $\dot{m}_{\text{P,ocean}} < [11, 100]\,\text{Tg/a}$. This PB is already in the right format and can be measured through the direct LCA inventory results P and PO_4 to ocean, soil, air and freshwater. P to ocean includes all P and PO_4 emissions to ocean, soil, freshwater, and air following the fate model employed in ReCiPe (Huijbregts et al., 2017), as proposed by Doka (2016). This fate model characterizes non-marine P emissions to direct marine P emissions by calculating the fraction of P arriving in the oceans. For example, one kilogram of P emission to soil in this fate model leads to 0.337 kg P in the ocean. The uncertainty range is directly taken from the inventory result. Dao et al. (2015) define an alternative boundary for P fertiliser application, which is contradicting the boundary for P to soil and therefore not considered here.

2.5.2 Phosphorus to soil

Applying mined P fertiliser on agricultural soil is the main driver for disturbed biogeochemical flows. The PB for applying mined phosphorus on agricultural soil is $\dot{m}_{\text{P,soil}} < [6.2, 11.2]\,\text{Tg/a}$.

The impact can be measured again from the LCA inventory results, this time for soil only as it specifically specifies application on soil. Following the precautionary principle, emissions on all soil types (i.e., industrial, agricultural, unspecified) in ecoinvent are considered, to account for unclear labeling and potential missing categories in agricultural soil (e.g., home gardening, infrastructure areas).

2.5.3 Industrial and intentional biological fixation of nitrogen

The nitrogen cycle is another biogeochemical cycle which is significantly changed by human activities. Therefore the PB specifies the limit on the industrial (e.g., Haber-Bosch fixation of N from air) and intentional biological fixation (e.g., through crops) of N to $\dot{m}_{\text{N}} < [62, 82]\,\text{Tg/a}$.

Assuming that all fixed nitrogen is sooner or later emitted as reactive nitrogen back to the environment, it is possible to count the reactive N emissions from inventory flows (Doka, 2016). This step is necessary as the intentional biological fixation of N is not directly accounted in LCIs. A list of reactive N compounds can be found in (Doka, 2016), which are converted into N-equivalents based on the molecular N content.

2.6 Landsystem change

2.6.1 Land use

Landsystem change is a major driver for species loss (Newbold et al., 2016; IRP, 2019; Dinerstein et al., 2017) and climate change (Snyder et al., 2004) but also an essential production factor for agriculture, renewable energy systems and infrastructure. Based on an assessment of the removal of natural land cover (Ramankutty and Foley, 1999) on the climate system (Snyder et al., 2004), the PB define the maximum land system change as remaining forest area (Steffen et al., 2015):

$$\frac{\text{area of forest}}{\text{area of original forest}} > \begin{cases} [75, 54]\% & \text{global average} \\ [85, 60]\% & \text{tropical or boreal forest biomes} \\ [50, 30]\% & \text{temporal forest biomes} \end{cases}$$

The PB restrict the remaining forest area only, thus leaving the question open how much of the other biomes can be used for human activities. In LCA land use in former forest biomes is usually not accounted

separately. Still, Ryberg et al. (2018) defines the boundary only for forest area ($< [1.6, 2.9] \times 10^{13}\,\mathrm{m}^2$), whereas Doka (2016) assumes all biomes other than forest to be completely appropriable and sets the boundary to $< [8.5, 9.3] \times 10^{13}\,\mathrm{m}^2$. Bjørn and Hauschild (2015) proposes a different boundary ($< 1.04 \times 10^{14}\,\mathrm{m}^2$) based on minimum area requirement for species conservation on all biomes equally, omitting the more strict boundaries for forests (which are based on climate sensitivity). Because of those limitations, we follow the approach in our previous work (Desing et al., 2019), combining the forest boundaries with the *nature needs half* proposal (Dinerstein et al., 2017) for the remaining biomes.The total land boundary can be estimated to be $A_{\mathrm{appr},p=0.98} = (6.01 \pm 0.924) \times 10^{13}\,\mathrm{m}^2/\mathrm{a}$ (see table S3).

biome	appropriable share of land area biome according to *biodiv*	according to *PB*	combined	appropriable land area $A_{\mathrm{appr},p=0.98}/10^{12}\,\mathrm{m}^2$
tropical forest	0.5	[0.15, 0.4]	[0.15, 0.5]	6.22 ± 2.77
temporal forest	0.5	[0.5, 0.8]	[0.5, 0.8]	11.1 ± 2.51
boreal forest	0.5	[0.15, 0.4]	[0.15, 0.5]	4.31 ± 1.92
others (excl. polar and RoL)	0.5	?	0.5	36.6 ± 0.18
sum			[0.35, 0.48]	60.1 ± 9.24

Table S3: Combination of *PB* (Steffen et al., 2015) and biodiversity conservation targets (*biodiv*) (Dinerstein et al., 2017) to form a boundary for land system change across all biomes. Table reproduced from earlier work (Desing et al., 2019).

For measuring land occupation, different land occupation categories from LCI (i.e., agriculture, industrial,...) are summed together. The uncertainty is defined through the basic uncertainty of the inventory flows.

2.6.2 Cropland use

The first publication on PB (Rockström et al., 2009) specifies that total cropland may not occupy more than $< [0.15, 0.2]$ of the ice-free land surface, which translates into $\dot{m}_{\mathrm{land,crop}} = [1.94, 2.61] \times 10^{13}\,\mathrm{m}^2/\mathrm{a}$. This boundary does not consider land conversion to pasture or infrastructure. This approach has been also used by Dao et al. (2015). Cropland occupation is a inventory category and can be directly measured. The uncertainty is taken from the ecoinvent inventory results.

2.7 Freshwater use

Freshwater consumed from the blue water stream is no longer available for freshwater ecosystems and further changes the hydrologial cycle. The PB for blue water consumption is set to $\dot{m}_{\mathrm{w,global}} = [4000, 6000] \times \mathrm{km}^3/\mathrm{a}$. The withdrawal and immediate or delayed discharge into the river also has an effect on the freshwater ecosystem, especially in low flow months. Thus an additional, regional and temporal explicit control variable is set for river basins with

$$\frac{\text{monthly withdrawal}}{\text{mean monthly river flow}} < \begin{cases} [25, 55]\% & \text{low flow months} \\ [30, 60]\% & \text{intermediate flow months} \\ [55, 85]\% & \text{high flow months} \end{cases}$$

The global blue water consumption boundary is already in the suitable format and can be adopted without changes (Ryberg et al., 2018; Doka, 2016). Meyer and Newman (2018) propose a boundary that also includes grey and green water consumption, which can be implemented in the future. Bjørn and Hauschild (2015) redefine the boundary based on environmental flow requirements and water stress. The regional withdrawal boundary requires a regionalized assessment, which we have excluded in the case study. There are ongoing efforts to define refined boundaries for freshwater (Gleeson et al., 2020; Zipper et al., 2020), which can be implemented once available.

Blue water consumption is an explicit elementary flow in Exiobase, however not in ecoinvent. Blue water consumption for LCI is thus approximated as the sum of all water emissions to air (i.e., evaporative

water consumption) (Doka, 2016). Note, that these emissions also include water formed in combustion processes and excludes water which is incorporated in products.

2.8 Atmospheric aerosol loading

Aerosols have a dimming effect on the climate system, but also change precipitation and wind patterns and have a negative effect on human and ecosystem health. The control variable is defined as the Aerosol Optical Depth (AOD), which correlates to the opacity of the atmosphere, and the PB is set for South Asia to $AOD < [0.25, 0.5]$. In South Asia, there is a background AOD of 0.15 (Steffen et al., 2015), thus defining an anthropogenic increase of AOD to $[0.1, 0.35]$. This boundary is not considered, as for the first application of the method we do not consider regionalized boundaries or impacts.

2.9 Novel entities

Novel materials and engineered organisms pose thread to ecosystems and human health, however there is no global boundary control variable defined yet (Rockström et al., 2009; Steffen et al., 2015).

Toxicological effects are indirectly considered in the biodiversity boundary. Doka (2016) suggests to set a boundary for disability adjusted life years based on the effect of novel entities on human health. Meyer and Newman (2018) propose a boundary for imperishable waste, which cannot be quantified in LCA and EE-IOT yet. For the proof of concept of the method, this PB is not integrated but a potential area of future research.

2.10 Energy

CE aims at closing material cycles, which becomes increasingly energy intensive with higher recycling rates (Baum, 2018). Thus the availability of sustainable energy may become a limiting factor for CE. A global boundary for renewable energy availability is therefore derived in an earlier paper (Desing et al., 2019), based on estimations for sustainable energy budgets for different RE resources. The RE boundary is estimated to be $ATP_{el,p=0.98} = (1.52^{+1.24}_{-0.81}) \times 10^{14}$ W (Desing et al., 2019). In a refined assessment, boundaries can be set for each RE resource separately.

The cumulative energy demand (CED) is a commonly used impact method in LCIA. The CED adds up all energy values of inventory results for energy carriers (chemical energy) and electricity provided by renewable energy resources (e.g., wind, solar but not biomass). To be inline with the boundary in electric energy, the CED values need to be converted to electricity equivalents. Therefore common conversion efficiencies are assumed for each reported energy carrier category (Desing et al., 2019).

Energy carrier inventory result in ecoinvent 3.5	unit	conversion efficiency	CF to CED_{el}/MJ
Energy, potential (in hydropower reservoir), converted	MJ	1	1
Energy, solar, converted	MJ	1	1
Energy, kinetic (in wind), converted	MJ	1	1
Energy, gross calorific value, in biomass	MJ	0.25	0.25
Energy, gross calorific value, in biomass, primary forest	MJ	0.25	0.25
Gas, natural, in ground	m^3	0.4	15.32
Oil, crude, in ground	kg	0.37	16.95
Peat, in ground	kg	0.34	3.37
Uranium, in ground	kg	0.33	186480
Coal, hard, unspecified, in ground	kg	0.34	6.49
Coal, brown, in ground	kg	0.34	3.37
Energy, geothermal, converted	MJ	1	1
Gas, mine, off-gas, process, coal mining	m^3	0.4	15.92

Table S4: Characterization factors (CF) for cumulative energy demand in electricity equivalents CED_{el} based on CF of CED in ecoinvent v.3.5 (Wernet et al., 2016) and conversion efficiencies to electricity from Cullen and Allwood (2010).

In Exiobase the total energy use is reported. This value lacks detail on energy carrier types however for a specific year the global energy mix is known (International Energy Agency, 2018) and it is thus possible to calculate an overall global "efficiency" of energy conversion to electricity equivalents.

$$\eta_{\text{overall,el}} = \frac{5.3 \times 10^{12}\,\text{W}_{\text{el}}}{1.8 \times 10^{13}\,\text{W}} = 0.29 \tag{4}$$

Assuming an uniform energy mix for all sectors, the conversion to electricity equivalents does not have an influence on the share of energy need for different sectors, only on the total.

3 Measuring impacts from industrial sectors with Exiobase

Exiobase is an EE-IOT for the global economy. It reports monetary flows from industries to industries to produce a final output to the society. For each of the 163 industries in the 43 countries and 6 rest of the world regions, the direct impacts caused are reported in the environmental extensions. We use Exiobase to calculate the global environmental impacts of the ESB categories and the impact share of resource production. In this way, we can allocate the ESB to resources. The definition of resource segments can be found in tab "S" in file "SoSOS_materials.xlsx" in the code files online https://doi.org/10.5281/zenodo.3629366.

3.1 ESB impact characterization method for Exiobase

Exiobase version 3 does not provide any impact characterization methods, but raw environmental flow data. These flows have to be translated into the PB impact categories using a characterization matrix $\boldsymbol{Q}$.

A characterization matrix $\boldsymbol{Q}$ is build to translate the flows into impacts for the PB categories (see sec.2). This impact assessment is based on ReCiPe v1.13 2016 (Huijbregts et al., 2017) and, for global warming potential, on the CREEA impact characterization factors provided with Exiobase version 2.2.2 (Tukker et al., 2009), which is based on LCIA methods such as CML 2001, ecoindicator 99 and usetox. Several PB categories only require elementary flows, which are directly taken from the flow matrix. The uncertainty range for impact characterization factors are modeled as uniform distributions with the minimum and maximum values among the respective impact assessment methods for each boundary. To also consider the uncertainty of the flows, $\boldsymbol{Q}_{IA}$ is multiplied with normalized uncertainty distribution (i.e., $mean = 1$) for each elementary flow, modeled as log-normal distribution. Exiobase doesn't provide information on the uncertainty range, thus it is assumed, that the uncertainty of inventory flows is similar to the corresponding uncertainty in ecoinvent (Ecoinvent, 2013).

$$\boldsymbol{Q} = \begin{matrix} n_{\text{flows}}\downarrow \\ 1 \\ \vdots \\ 1104 \end{matrix} \begin{matrix} \begin{matrix} 1 & & n_{\text{flows}} & & 1104 \end{matrix} \\ \begin{bmatrix} 1e^{\pm\sigma_1} & & & & 0 \\ & & \ddots & & \\ 0 & & & & 1e^{\pm\sigma_{1104}} \end{bmatrix}_{\ddots_{n_{\text{runs}}}} \end{matrix} \times \begin{matrix} flows\downarrow \\ 1 \\ \vdots \\ 1104 \end{matrix} \begin{matrix} \begin{matrix} 1 & n_{\text{PB}} & 11 \end{matrix} \\ \begin{bmatrix} & & \\ & \boldsymbol{Q}_{IA} & \\ & & \end{bmatrix}_{\ddots_{n_{\text{runs}}}} \end{matrix} \tag{5}$$

3.2 Analyzing direct impacts from industries

The direct emissions resulting in the target segments (i.e., material related industries) can be calculated by adding up all environmental impacts of relevant industries. In the environmental extensions, emissions and resource flows (hereafter called "flows") are reported in the matrices $\boldsymbol{f}$ (flows for each product and country) and $\boldsymbol{f}_{\text{hh}}$ (flows for each final demand (FD) category (hh = household) and country. The flows for each product in the different countries $n_{\text{country}} = 49$ has to be summed up to result in global totals, reducing the product dimension from 7987 to 163 (eq. 6) and the FD dimension from 343 to 7 (eq. 7). The two flow matrices are combined to a single one in eq. 8.

$$\boldsymbol{f}_{\text{industry}}(i) = \sum_{k=1}^{n_{\text{country}}} f_x((i + n_{\text{industry}}(k-1)) \qquad \forall i = 1 \dots n_{\text{industry}} \tag{6}$$

$$\boldsymbol{f}_{FD}(i) = \sum_{k=1}^{n_{\text{country}}} f_{\text{hh}}((i + n_{\text{hh}}(k-1)) \qquad \forall i = 1 \dots n_{\text{FD}} \tag{7}$$

$$\boldsymbol{f} = \left[\begin{array}{c|c} \boldsymbol{f}_{\text{industry}} & \boldsymbol{f}_{\text{FD}} \end{array} \right] \tag{8}$$

These direct impacts, however do not include impacts caused by inputs in this segment from the rest of economy, e.g., electricity.

3.3 Including supply chain impacts

The approach chosen here (Dente et al., 2018; Cabernard et al., 2019a,b), isolates the target industries (i.e., the outputs form industries of interest, here: primary material production) from the rest of the economy (RoE). It then allocates all environmental impacts from inputs from target and non-target industries to the final output of the target industries. e.g., steel (itself a target industry) necessary to produce aluminum, such as for production infrastructure, is allocated to the aluminum output as is required electricity (non-target industry). The procedure effectively allocates all upstream environmental impacts to the output of a target industry, supplied to the RoE and FD.

The total demand $\vec{\boldsymbol{x}}$ is calculated from an input-output table $\boldsymbol{A}$ and the FD $\boldsymbol{y}$. The FD is reported in 7 categories for the $n_{\text{countries}} = 49$ countries and rest-of-world regions. The overall FD is then the sum over all categories, which results in a FD vector $\vec{\boldsymbol{y}}$. Per country $n_{\text{industry}} = 163$ different industry categories are reported.

$$\begin{aligned} \vec{\boldsymbol{x}} &= \boldsymbol{A} \times \vec{\boldsymbol{x}} + \vec{\boldsymbol{y}} \\ \vec{\boldsymbol{x}} &= (\boldsymbol{I} - \boldsymbol{A})^{-1} \times \vec{\boldsymbol{y}} = \boldsymbol{L} \times \vec{\boldsymbol{y}} \end{aligned} \tag{9}$$

The values of $\vec{\boldsymbol{x}}$ express the total output of each industry and region, including the output supplied to other industries. In order to calculate the output of the target segment of the economy, without double counting the output which is consumed within the target segment itself, the whole input-output table is split into target (t) and other (o) industries (Dente et al., 2018).

$$\boldsymbol{A} = \begin{bmatrix} \boldsymbol{A}_{tt} & \boldsymbol{A}_{to} \\ \boldsymbol{A}_{ot} & \boldsymbol{A}_{oo} \end{bmatrix} \qquad \boldsymbol{L} = \begin{bmatrix} \boldsymbol{L}_{tt} & \boldsymbol{L}_{to} \\ \boldsymbol{L}_{ot} & \boldsymbol{L}_{oo} \end{bmatrix} \qquad \boldsymbol{L}_{all-t} = \begin{bmatrix} \boldsymbol{L}_{tt} \\ \boldsymbol{L}_{ot} \end{bmatrix} \tag{10}$$

The overall production volume of each industry within the target segment $\vec{\boldsymbol{x}}_t$ needs to equal the production necessary to supply the final output of the segment $\vec{\boldsymbol{x}}_{t,wdc}$ (wdc... without double counting). This output of the segment is required by direct FD $\vec{\boldsymbol{y}}_t$ and by the requirements of the ROE to produce the FD from all other industries $\vec{\boldsymbol{y}}_o$ (Cabernard et al., 2019a).

$$\vec{\boldsymbol{x}}_t = \boldsymbol{L}_{tt} \times \vec{\boldsymbol{x}}_{t,wdc} \tag{11}$$

$$\vec{\boldsymbol{x}}_{t,wdc} = \vec{\boldsymbol{y}}_t + \boldsymbol{A}_{to} \times \boldsymbol{L}_{oo}^{T} \times \vec{\boldsymbol{y}}_o \tag{12}$$

Environmental extensions are reported in Exiobase in elementary flow matrices $\boldsymbol{f}$ for the total production output $\vec{\boldsymbol{x}}$ and $\boldsymbol{f}_{\text{FD}}$ for the FD $\vec{\boldsymbol{y}}$. The emission intensity $\boldsymbol{F}$ for each industry can then be calculated by dividing each column in $\boldsymbol{f}$ with the respective total production output. Finally, the elementary flows associated with production of the segment's output is calculated in eq. 13.

$$\boldsymbol{f}_{t,wdc} = \boldsymbol{F} \times \boldsymbol{L}_{all-t} \times \hat{\boldsymbol{x}}_{t,wdc} \tag{13}$$

$$\underbrace{\begin{bmatrix} \\ \boldsymbol{f}_{t,wdc} \\ \\ \end{bmatrix}}_{1104\times n_t} = \underbrace{\begin{bmatrix} \\ \boldsymbol{F} \\ \\ \end{bmatrix}}_{1104\times 7987} \times \underbrace{\begin{bmatrix} \\ \boldsymbol{L}_{all-t} \\ \\ \end{bmatrix}}_{7987\times n_t} \times \underbrace{\begin{bmatrix} \ddots & & 0 \\ & x_{t,wdc}(i) & \\ 0 & & \ddots \end{bmatrix}}_{n_t\times n_t}$$

The total elementary flows for the whole world economy is simply the sum over all industries, FD categories and regions. The flows for the ROE is then the difference between the FD and target segment from the total flows.

$$\boldsymbol{f}_{total} = sum(\boldsymbol{f}, 2) + sum(\boldsymbol{f}_{FD}, 2) \tag{14}$$

$$\boldsymbol{f}_{RoE} = \boldsymbol{f}_{total} - sum(\boldsymbol{f}_{t,wdc}, 2) - sum(\boldsymbol{f}_{FD}, 2) \tag{15}$$

$$\tag{16}$$

Industries can be grouped into sectors using a sector matrix $\boldsymbol{S}$. The target segment "materials", as the subject of this study, consists of multiple sectors, which are groupings of industries by material classes (e.g., metals, construction materials,...). Each industry can only be assigned to one sector to avoid double counting. Note, that the sectors can be assembled in different ways, which is subject to the modeler's choice.

$$\boldsymbol{f}_{sector} = \boldsymbol{f}_{t,wdc} \times \boldsymbol{S} \tag{17}$$

The impacts on the PB categories are calculated as follows:

$$\boldsymbol{q}_{t,wdc/FD/total} = \boldsymbol{Q}^T \times \boldsymbol{f}_{t,wdc/FD/total} \tag{18}$$

The impact results are then further converted into relative shares, i.e., the share of the impact from one product or sector in relation to the total impact by all products/sectors is determined.

$$\boldsymbol{SoSOS}_{t,wdc} = \frac{\boldsymbol{q}_{t,wdc}}{\boldsymbol{q}_{total}} \tag{19}$$

$$\boldsymbol{SoSOS}_{sector} = \boldsymbol{SoSOS}_{t,wdc} \times \boldsymbol{S} \tag{20}$$

3.4 Calculation of the oversize factor

By calculating the supply chain impacts for the target segment, all impacts associated with the final output to the rest of the economy are accounted to the final output. This final output is, however, lower than the overall production in the respective target industry, as this industry also supplies materials to other target industries. For example, steel is not only used in the RoE, but also to produce plastics. The supply chain impacts for plastics already include the impacts associated to the steel necessary for plastic production. Through the double-counting correction procedure (Cabernard et al., 2019b; Dente et al., 2018), the output of steel is reduced by the amount required in plastics. Therefore, the overall production in each target industry needs to be larger than the final output to the RoE by the oversize factor:

$$\omega = \frac{\dot{m}_{\text{overall production}}}{\dot{m}_{\text{production output}}} \tag{21}$$

$$= \frac{\vec{\boldsymbol{x}}_t}{\vec{\boldsymbol{x}}_{t,wdc}} \tag{22}$$

4 ESB impact calculation and process selection in ecoinvent

Many ESB can be measured with inventory results directly (CO_2 emissions, P to ocean, P to soil, N emissions, land-use, and blue water consumption). For these impacts, the uncertainty is modelled with a log-normal distribution with the variance provided in the ecoinvent quality guideline (Ecoinvent, 2013). For all other boundaries, which require impact assessment methods, the uncertainty is combined as the inventory uncertainty and a rectangular distribution for the variation of different LCIA methods. For all boundaries, used LCIA methods and LCI uncertainty function are listed in table S5.

Impact categories	Unit	LCIA method	Uncertainty distribution
Direct CO_2 emission to air	kg CO_2	-	Log-normal
Global warming potential	kg $CO_{2,eq}$	CML 2001, ILCD 2.0 2018, IPCC 2007, IPCC, 2013, ReCiPe 2016	Uniform
Potentially disappeared species	species.years	3 scenarios of ReCiPe 2016	Uniform
Ozone depletion potential	kg $CFC_{10,eq}$	CML 2001, ILCD 2.0 2018, ReCiPe 2016	Uniform
Phosphorus to ocean	kg P	-	Log-normal
Phosphorus to soil	kg P	-	Log-normal
Nitrogen emission	kg N	-	Log-normal
Land-use	m^2a	-	Log-normal
Water emission to air	m^3	-	Log-normal
Cumulative energy demand	MJ eq	-	Log-normal

Table S5: Impact categories selection, characterization, and uncertainty models

For the ERA method, the impacts resulting from extraction, processing and final treatment of the resources is required. Therefore, representative processes from the ecoinvent database have to be selected. The cut-off system model has been used (Wernet et al., 2016) so that cumulative impacts for processed material already includes the impacts of the up-stream supply chain (i.e. mining, transportation, processing) and the impacts for final treatment start with the point where the resource becomes final waste. The selected processes for the case study are listed in table S6. Because the case study on the ERA method aims to calculate global resource budgets, the requirement is to choose global production and waste treatment processes from the ecoinvent data-base.

Ecoinvent often reports country or region specific production processes only. Thus, global weighted averages are formed based on multiple production/ waste treatment processes available in ecoinvent for a specific material. For example, the process *primary production of aluminum (ingot)* exists in ecoinvent for ten countries/ regions. The global average impacts for this process can therefore be weighted with their respective market share.

Metal	Primary production	Incineration
Aluminum	Aluminum, primary, ingot (China; Africa; Asia w/o China; EU; Gulf council; Russia; South America; Northern America; Oceania; Rest of the World)	Scrap aluminum, incineration (Switzerland; EU; Rest of the World)
Copper	Copper production, primary (Australia; Asia; Europe; Latin America and the Caribbean; Northern America; Rest of the World)	Scrap copper, incineration (Switzerland; EU; Rest of the World)
Steel	Steel production, unalloyed, converter (Europe; Rest of the World)	Scrap steel, incineration (Switzerland; EU; Rest of the World)
Cast iron	Cast iron production (Europe; Rest of the World)	Scrap steel, incineration (Switzerland; EU; Rest of the World)
Zinc	Market for zinc (global)	Treatment of hazardous waste, hazardous waste incineration (global)
Lead	Primary lead production from concentrate (global)	Treatment of hazardous waste, hazardous waste incineration (global)
Tin	Market for tin (global)	Treatment of scrap tin sheet, municipal incineration (global)
Nickel	Market for nickel (global)	Treatment of hazardous waste, hazardous waste incineration (global)
Gold	Market for gold (global)	Treatment of hazardous waste, hazardous waste incineration (global)
Silver	Market for silver (global)	Treatment of hazardous waste, hazardous waste incineration (global)
Platinum	Market for platinum (global)	Treatment of hazardous waste, hazardous waste incineration (global)
Titanium	Market for titanium, primary (global)	Treatment of hazardous waste, hazardous waste incineration (global)
Chromium	Market for chromium (global)	Treatment of hazardous waste, hazardous waste incineration (global)
Stainless steel	Chromium steel 18/8, hot rolled (global)	Scrap steel, incineration (Switzerland; EU; Rest of the World)

Table S6: Ecoinvent processes for selected metals

5 Glossary and abbreviations

term	description
Availability	The fact that something can be used, or utilized (e.g., by the Earth system or humanity)
Circular Economy	The Circular Economy is a model adopting a resource-based and systemic view, aiming at taking into account all the variables of the system earth, in order to maintain its viability for human beings. It serves the society to achieve well-being within the physical limits and planetary boundaries. It achieves that through technology and business model innovation, which provide the goods and services required by society, leading to long term economic prosperity. These goods and services are powered by renewable energy and rely on materials which are either renewable through biological processes or can be safely kept in the technosphere, requiring minimum raw material extraction and ensuring safe disposal of inevitable waste and dispersion in the environment. CE builds on and manages the sustainably available resources and optimizes their utilization through minimizing entropy production, slow cycles and resource and energy efficiency. (Desing et al., 2020)
Earth System	The entirety of Earth's interacting physical, chemical and biological processes
Earth System Boundaries	Limits to Earth system processes that, if crossed, significantly disturb the interacting web of processes with potential to trigger fast and irreversible change to a new equilibrium.
Emission budget	The quantification of the PB to to annual emission allowances. If the socio-economic system does not emit/ extract more than the budgets allow, it can be considered sustainable in the long run
Final demand	Comprises the purchase and use of goods and services by the end-consumer (e.g., household) in the Exiobase database
Industry	A single industry in the Exiobase database (e.g., iron ore extraction)
Planetary Boundaries	A specific set of Earth System Boundaries compromising nine planetary processes
State-of-the-art technology	Widely used technology, available in the market in various different products
Resource	The smallest unit in the ERA method representing a stock of one material
Resource budget	The maximum annual production of a resource which does not exceed its assigned emission budgets
Resource segment	Includes all industries in the Exiobase database that produce the same kind of material (e.g., aluminum is part of the metal segment)
Rest of economy	Holds all activities of the Exiobase database that are not part of any resource production value chain (e.g., manufacturing of end-user devices)
Safe Operating Space	Environmental impacts that can be safely exerted on the Earth system, without risking (i.e., with very low probability) the destabilization of the Earth System due to human interference. Synonym for carrying capacity
Share of Safe Operating Space	Relative part of the global Safe Operating Space allocated to a production or consumption activity (e.g., 30 % of nitrogen allowance level assigned to agriculture)
Segment Boundary	Boundary value assigned to an activity (e.g., 10 tons of phosphorus assigned to textile sector); needs to be smaller than global boundary ($SB \leq ESB$).

term	description
Share of production	The relative production share of one single material to a combination of similar materials. For example, steel's share of production of the metal sector is about 90 %

The following abbreviations are used in this paper:

ATP	appropriable technical potential
AOD	aerosol optical depth
BII	biodiversity intactness index
CE	Circular Economy
CED	Cumulative energy demand
DU	Dobson Units
EE-IOT	Envionmentally extended input output table
EoL	End of life
ERA	Ecological Resource Availability
ESB	Earth system boundaries
FD	Final demand
GWP	global warming potential
LCA	Life Cycle Assessment
LCI	Life Cycle Inventories
LCIA	Life Cycle Impact Assessment
MC	Monte Carlo simulation
PB	Planetary Boundaries
PDF	Probability density function
PM	particulate matter
ODP	Ozone depletion potential
ODS	ozone depleting substance
RE	renewable energy
RoE	Rest of economy
RoL	rest of land
SB	Segment boundary
SM	Supplementary materials
SoP	Share of production
SOS	Safe Operating Space
SoSOS	Share of Safe Operating Space
UI	Unit impacts

References

Baum, H.-G. (2018). Eco-efficiency - a measure to determine optimal recycling rates? In Fellner, J., Laner, D., and Lederer, J., editors, Science to support Circular Economy. Christian Doppler Laboratory "Anthropogenic Resources", TU Wien Institute for Water Quality and Resource Management,.

Bjørn, A. and Hauschild, M. Z. (2015). Introducing carrying capacity-based normalisation in lca: framework and development of references at midpoint level. The International Journal of Life Cycle Assessment, 20(7):1005–1018.

Cabernard, L., Pfister, S., and Hellweg, S. (2019a). Data and tool for: A new method for analysing supply chain impacts and application to global material resources.

Cabernard, L., Pfister, S., and Hellweg, S. (2019b). A new method for analyzing sustainability performance of global supply chains and its application to material resources. Sci Total Environ, 684:164–177.

Chandrakumar, C., McLaren, S. J., Jayamaha, N. P., and Ramilan, T. (2018). Absolute sustainability-based life cycle assessment (aslca): A benchmarking approach to operate agri-food systems within the 2 degree c global carbon budget. Journal of Industrial Ecology, 23(4):906–917.

Cullen, J. M. and Allwood, J. M. (2010). Theoretical efficiency limits for energy conversion devices. Energy, 35(5):2059–2069.

Dao, H., Peduzzi, P., Chatenoux, B., De Bono, A., Schwarzer, S., and Friot, D. (2015). Environmental limits

and swiss footprints based on planetary boundaries. Report, UNEP/GRID-Geneva, University of Geneva, Swiss Federal Office for the Environment (FOEN).

Dao, H., Peduzzi, P., and Friot, D. (2018). National environmental limits and footprints based on the planetary boundaries framework: The case of switzerland. Global Environmental Change, 52:49–57.

Dente, S. M. R., Aoki-Suzuki, C., Tanaka, D., and Hashimoto, S. (2018). Revealing the life cycle greenhouse gas emissions of materials: The japanese case. Resources, Conservation and Recycling, 133:395–403.

Desing, H., Brunner, D., Takacs, F., Nahrath, S., Frankenberger, K., and Hischier, R. (2020). A circular economy within the planetary boundaries: Towards a resource-based, systemic approach. Resources, Conservation and Recycling, 155.

Desing, H., Widmer, R., Beloin-Saint-Pierre, D., Hischier, R., and Wäger, P. (2019). Powering a sustainable and circular economy—an engineering approach to estimating renewable energy potentials within earth system boundaries. Energies, 12(24).

Dinerstein, E., Olson, D., Joshi, A., Vynne, C., Burgess, N. D., Wikramanayake, E., Hahn, N., Palminteri, S., Hedao, P., Noss, R., Hansen, M., Locke, H., Ellis, E. C., Jones, B., Barber, C. V., Hayes, R., Kormos, C., Martin, V., Crist, E., Sechrest, W., Price, L., Baillie, J. E. M., Weeden, D., Suckling, K., Davis, C., Sizer, N., Moore, R., Thau, D., Birch, T., Potapov, P., Turubanova, S., Tyukavina, A., de Souza, N., Pintea, L., Brito, J. C., Llewellyn, O. A., Miller, A. G., Patzelt, A., Ghazanfar, S. A., Timberlake, J., Kloser, H., Shennan-Farpon, Y., Kindt, R., Lilleso, J. B., van Breugel, P., Graudal, L., Voge, M., Al-Shammari, K. F., and Saleem, M. (2017). An ecoregion-based approach to protecting half the terrestrial realm. Bioscience, 67(6):534–545.

Doka, G. (2016). Combining life cycle inventory results with planetary boundaries: The planetary boundary allowance impact assessment method. update pba'06. Report, Doka Life Cycle Assessment.

Ecoinvent (2013). Ecoinvent v3 data quality guideline. Report, Ecoinvent.

EEA and FOEN (2020). Is europe living within the limits of our planet? - an assessment of europe's environmental footprints in relation to planetary boundaries. Report, European Environmental Agency, Swiss Ferderal Office for the Environment,.

European Commission (2011). Our life insurance, our natural capital: an eu biodiversity strategy to 2020. Report COM(2011) 244 final, European Union,.

Gleeson, T., Wang-Erlandsson, L., Zipper, S. C., Porkka, M., Jaramillo, F., Gerten, D., Fetzer, I., Cornell, S. E., Piemontese, L., Gordon, L. J., Rockström, J., Oki, T., Sivapalan, M., Wada, Y., Brauman, K. A., Flörke, M., Bierkens, M. F. P., Lehner, B., Keys, P., Kummu, M., Wagener, T., Dadson, S., Troy, T. J., Steffen, W., Falkenmark, M., and Famiglietti, J. S. (2020). The water planetary boundary: Interrogation and revision. One Earth, 2(3):223–234.

Goedkoop, M., Heijungs, R., Huijbregts, M. A., De Schryver, A., Struijs, J., and Van Zelm, R. (2013). Recipe 2008 - a lcia method which comprises harmonised category indicators at the midpoint and the endpoint level. Report, Ministry of Housing, Spatial Planning and Environment, The Netherlands.

Heuler, P., Frost, M., and Rochlitz, H. (2010). Load assumptions for durability assessment of automotive structure. Engineering Integrity, 29:8–19.

Huijbregts, M., Steinmann, Z., Elshout, P., Stam, G., Verones, F., Vieira, M., Zijp, M., Hollander, A., and van Zelm, R. (2017). Recipe2016 - a harmonised life cycle impact assessment method at midpoint and endpoint level. International Journal of Life Cycle Assessment, 22:138–147.

Hupfer, A. (2011). Konstruktionsaspekte bei flugantrieben. Report, Technische Universität München (TUM).

International Energy Agency (2018). Energy balance for the world, 2015.

IPBES (2019). Global assessment report on biodiversity and ecosystem services of the intergovernmental science-policy platform on biodiversity and ecosystem services. Report, Secretariat of the Intergovernmental Science-Policy Platform on Biodiversity and Ecosystem Services.

IPCC (2013). Assessment report 5: Climate change 2013, the physical science basis. Report, IPCC.

IRP (2019). Global resources outlook. Report, UNEP.

Mace, G. M., Reyers, B., Alkemade, R., Biggs, R., Chapin, F. S., Cornell, S. E., Díaz, S., Jennings, S., Leadley, P., Mumby, P. J., Purvis, A., Scholes, R. J., Seddon, A. W. R., Solan, M., Steffen, W., and Woodward, G. (2014). Approaches to defining a planetary boundary for biodiversity. Global Environmental Change, 28:289–297.

Meyer, K. and Newman, P. (2018). The planetary accounting framework: a novel, quota-based approach to understanding the impacts of any scale of human activity in the context of the planetary boundaries. Sustainable Earth, 1(1).

Molland, A. F. (2008). The Maritime Engineering Reference Book. The Maritime Engineering Reference Book. Butterworth-Heinemann, Oxford.

Montoya, J. M., Donohue, I., and Pimm, S. L. (2018). Planetary boundaries for biodiversity: Implausible science, pernicious policies. Trends Ecol Evol, 33(2):71–73.

Muller, S., Lesage, P., Ciroth, A., Mutel, C., Weidema, B. P., and Samson, R. (2014). The application of the pedigree approach to the distributions foreseen in ecoinvent v3. The International Journal of Life Cycle Assessment, 21(9):1327–1337.

Muller, S., Lesage, P., and Samson, R. (2016). Giving a scientific basis for uncertainty factors used in global life cycle inventory databases: an algorithm to update factors using new information. The International Journal of Life Cycle Assessment, 21(8):1185–1196.

Myhre, G., Shindell, D., Bréon, F.-M., Collins, W., Fuglestvedt, J., Huang, J., Koch, D., Lamarque, J.-F., Lee, D., Mendoza, B., Nakajima, T., Robock, A., Stephens, G., Takemura, T., and Zhang, H. (2013). Anthropogenic and Natural Radiative Forcing, book section 8. Cambridge Unversity Press, Cambridge.

Newbold, T., Hudson, L. N., Arnell, A. P., Contu, S., De Palma, A., Ferrier, S., Hill, S. L. L., Hoskins, A. J., Lysenko, I., Phillips, H. R. P., Burton, V. J., Chng, C. W. T., Emerson, S., Gao, D., Pask-Hale, G., Hutton, J., Jung, M., Sanchez-Ortiz, K., Simmons, B. I., Whitmee, S., Zhang, H. B., Scharlemann, J. P. W., and Purvis, A.

(2016). Has land use pushed terrestrial biodiversity beyond the planetary boundary? a global assessment. Science, 353(6296):288–291.

Ramankutty, N. and Foley, J. A. (1999). Estimating historical changes in global land cover: croplands from 1700 to 1992. Global Biochemical Cycles, 13(4):997–1027.

Rockström, J., Steffen, W., Noone, K., Persson, A., Chapin, S., Lambin, E., Lenton, T. M., Scheffer, M., Folke, C., Schnellhuber, H., Nykvist, B., De Wit, C. A., Hughes, T., van der Leeuw, S., Rodhe, H., Sörlin, S., Snyder, P., Costanza, R., Svedin, U., Falkenmark, M., Karlberg, L., Corell, R. W., Fabry, V., Hansen, J., Brian, W., Liverman, D., Richardson, K., Crutzen, P., and Foley, J. (2009). Planetary boundaries: Exploring the safe operating space for humanity. Ecology and Society, 14(2).

Ryberg, M. W., Owsianiak, M., Richardson, K., and Hauschild, M. Z. (2018). Development of a life-cycle impact assessment methodology linked to the planetary boundaries framework. Ecological Indicators, 88:250–262.

Sarmiento, J. and Gruber, N. (2006). Ocean geochemical cycles. Princton University Press.

Scholes, R. J. and Biggs, R. (2005). A biodiversity intactness index. Nature, 434(7029):45–9.

Snyder, P. K., Delire, C., and Foley, J. A. (2004). Evaluating the influence of different vegetation biomes on the global climate. Climate Dynamics, 23(3-4):279–302.

Stadler, K., Wood, R., Bulavskaya, T., Södersten, C.-J., Simas, M., Schmidt, S., Usubiaga, A., Acosta-Fernández, J., Kuenen, J., Bruckner, M., Giljum, S., Lutter, S., Merciai, S., Schmidt, J. H., Theurl, M. C., Plutzar, C., Kastner, T., Eisenmenger, N., Erb, K.-H., de Koning, A., and Tukker, A. (2018). Exiobase 3: Developing a time series of detailed environmentally extended multi-regional input-output tables. Journal of Industrial Ecology, 22(3):502–515.

Steffen, W., Richardson, K., Rockstrom, J., Cornell, S. E., Fetzer, I., Bennett, E. M., Biggs, R., Carpenter, S. R., de Vries, W., de Wit, C. A., Folke, C., Gerten, D., Heinke, J., Mace, G. M., Persson, L. M., Ramanathan, V., Reyers, B., and Sorlin, S. (2015). Sustainability. planetary boundaries: guiding human development on a changing planet. Science, 347(6223):1259855.

Stein, R. (1991). Accumulation of Organic Carbon in Marine Sediments. Lecture Notes in Earth Sciences. Springer.

Tukker, A., Bulavskaya, T., Giljum, S., de Koning, A., Lutter, S., Simas, M., Stadler, K., and Wood, R. (2014). The global resource footprint of nations. carbon, water, land and materials embodied in trade and final consumption calculated with exiobase 2.1. Report, Exiobase.

Tukker, A., Poliakov, E., Heijungs, R., Hawkins, T., Neuwahl, F., Rueda-Cantuche, J. M., Giljum, S., Moll, S., Oosterhaven, J., and Bouwmeester, M. (2009). Towards a global multi-regional environmentally extended input–output database. Ecological Economics, 68(7):1928–1937.

UNEP and SETAC (2016). Global guidance for life cycle impact assessment indicators - volume 1. Report ISBN 978-92-807-3630-4, UN environmental program, Life cycle initiative,.

Velders, G. J., Andersen, S. O., Daniel, J. S., Fahey, D. W., and McFarland, M. (2007). The importance of the montreal protocol in protecting climate. Proceedings of the National Academy of Sciences, 104(12):4814–4819.

Verones, F., Bare, J., Bulle, C., Frischknecht, R., Hauschild, M., Hellweg, S., Henderson, A., Jolliet, O., Laurent, A., Liao, X., Lindner, J. P., Maia de Souza, D., Michelsen, O., Patouillard, L., Pfister, S., Posthuma, L., Prado, V., Ridoutt, B., Rosenbaum, R. K., Sala, S., Ugaya, C., Vieira, M., and Fantke, P. (2017). Lcia framework and cross-cutting issues guidance within the unep-setac life cycle initiative. Journal of Cleaner Production, 161:957–967.

Volkmer, M. (2007). Kernenergie basiswissen. Report, Informationskreis KernEnergie.

Wernet, G., Bauer, C., Steubing, B., Reinhard, J., Moreno-Ruiz, E., and Weidema, B. (2016). The ecoinvent database version 3 (part i): overview and methodology. The International Journal of Life Cycle Assessment, 21(9):1218–1230.

Zipper, S. C., Jaramillo, F., Wang-Erlandsson, L., Cornell, S. E., Gleeson, T., Porkka, M., Häyhä, T., Crépin, A., Fetzer, I., Gerten, D., Hoff, H., Matthews, N., Ricaurte-Villota, C., Kummu, M., Wada, Y., and Gordon, L. (2020). Integrating the water planetary boundary with water management from local to global scales. Earth's Future, 8(2).